Resonant magnetic reflection coefficients at the Fe 2*p* edge obtained with linearly and circularly polarized soft x rays

H.-Ch. Mertins,* D. Abramsohn, A. Gaupp, F. Schäfers, and W. Gudat
BESSY GmbH, Albert-Einstein-Strasse 15, D-12489 Berlin, Germany

O. Zaharko and H. Grimmer
Laboratory for Neutron Scattering ETHZ & PSI, CH-5232 Villigen, Switzerland

P. M. Oppeneer
Institute of Solid State and Materials Research, P.O. Box 270016, D-01171 Dresden, Germany
(Received 15 February 2002; revised manuscript received 9 July 2002; published 5 November 2002)

A systematic study of the specular reflectivity using circularly and linearly polarized radiation on magnetic materials is presented. Within a frame work based on the complete reflection matrix and the Stokes parameter formalism, the reflectance is modeled as a function of the polarization state of the incoming light for the longitudinal and the transversal magnetization. The nonmagnetic reflection coefficients and their individual magnetic contributions are determined from resonant magnetic reflectivity experiments of polarized soft x rays across the Fe-2*p* absorption edge on a ferromagnetic Fe/C multilayer. Exploiting tunable undulator radiation the absolute reflectance is investigated as a function of the degree of circular or linear polarization, photon energy, angle of incidence, and magnetic-field direction. As predicted by the developed formalism the corresponding magnetic asymmetry parameters depend nonlinearly on the degree of polarization at large angles of incidence due to the influence of the polarizing power of the sample. In the longitudinal geometry using circularly polarized light, the magnetic contribution is directly related to the magnetic contribution of the optical constants, which have independently been determined by Faraday measurements on an identical transmission sample.

DOI: 10.1103/PhysRevB.66.184404 PACS number(s): 78.20.−e, 78.70.Dm

I. INTRODUCTION

Magneto-optical spectroscopy techniques in the x-ray range like the magnetic circular dichroism (XMCD),[1,2] the Faraday effect,[3–5] the magnetic linear dichroism (XMLD)[6,7] or the x-ray Voigt effect[8] have become leading-edge research methods in the investigation of both fundamental and applied aspects of magnetism using polarized light. These techniques allow for element selective investigations of magnetic materials[9,10] and for imaging of magnetic domain structures.[11–14] Thus they hold great potential for the investigation of new magnetic materials as technologically important magneto resistive, spin valve and exchange-biased materials.[15]

Among these spectroscopies resonant magnetic scattering and specular reflectometry of circularly and linearly polarized soft x rays[6,10,16–18] have gained increasing importance since the resonantly enhanced transmission probability at absorption edges leads to large magnetic responses. The relative amplitude of the dichroic effect can exceed that observed in XMCD absorption experiments. These large dichroic effects in reflection observable over a wide range of incident angle and their sensitivity to layer thickness and interface roughness can be exploited for the study of element-specific magnetic depth profiles of magnetic films or multilayers.[19–21]

Experiments of the specular magnetic reflectivity can be viewed as variants of the magneto-optical Kerr effect (MOKE) which can be realized in different geometries. The transversal Kerr effect (T-MOKE) is observed when light is reflected from a sample with its magnetic moments lying parallel to the surface plane and perpendicular to the plane of incidence. Commonly linearly polarized light with polarization vector in the plane of incidence (*p* geometry) is used. In the longitudinal geometry (L-MOKE) the magnetic moments are parallel to the plane of incidence and parallel to the sample surface. Circularly polarized light is used generally. As a measure for the magnetic contribution to the reflection coefficients, the asymmetry parameter $A=(I_+-I_-)/(I_++I_-)$ is used. It is defined from the reflected intensities for two antiparallel orientations of the magnetization M.[22] The asymmetry in reflection experiments is sensitive to the angle of incidence, to the polarization state of photons, to the individual structure of the sample, i.e., layer thickness or interface roughness[16–21] and, of course, also to the electronic band structure.[23] Knowledge of the dependence of the asymmetry on the polarization state of light is essential for a quantitative understanding of the magnetic dichroism. While for absorption experiments in the soft x-ray regime, such investigations exist,[24,25] to our knowledge only one experimental paper reports on the polarization dependence of scattered intensities in the L-MOKE geometry, focussing on the 3*p* edges of transition metals.[26] Several theoretical papers have been published on this topic. The nonresonant magnetic reflectivity is well understood and written in a practicable formalism that allows for an easy quantitative analysis of polarization-dependent reflectivity data.[27,28] Resonant magnetic reflectivity on the other hand is more complicated since second-order terms become important. Several groups have pointed out the usefulness of the reflectance matrix formal-

ism and used it to analyze the magnetic contribution to resonant soft x-ray reflectance in L- or T-MOKE geometry.[17,18,21,29–34] However, a detailed theoretical and experimental analysis of the resonant magnetic reflectivity as a function of the degree of linear or circular polarization is still missing.

In this paper we extend a formalism from the near-visible region into the soft x-ray region to describe the polarization dependence of resonant x-ray reflectivity in the L-MOKE and T-MOKE geometry. One of our aims is to determine the reflection coefficients from reflectivity experiments in various possible geometries which allows us to separate charge and magnetic contributions. Our formalism which is based on the reflection matrix and the Stokes formalism is developed in Sec. II. The experimental set up is discussed in Sec. III. In Sec. IV the reflectivity data on a Fe/C multilayer across the Fe-2*p* edge in L- and T-MOKE geometry are presented as a function of the degree of linear or circular polarization, angle of incidence, and magnetic field. The dependence of the asymmetry parameters on the polarization state of the incoming light is discussed. The reflection coefficients distinguishing between charge and magnetic contributions are determined in Sec. V.

II. THEORY

A. Reflectivity

In this section expressions are derived for the reflectivity and the magnetic asymmetry as a function of the polarization of the incident light, appropriate for L-MOKE, T-MOKE, and intermediate geometries. We choose the Cartesian coordinate systems $(\mathbf{x},\mathbf{y},\mathbf{k}/|k|)$ and $(\mathbf{x}',\mathbf{y}',\mathbf{k}'/|k'|)$ to describe the incoming and outgoing electromagnetic waves with their respective wave vectors $\mathbf{k}$, $\mathbf{k}'$ and the unit vectors $\mathbf{x}$, $\mathbf{y}$, $\mathbf{x}'$ and $\mathbf{y}'$, respectively. The reflected wave $\mathbf{E}'$ is given by the product of the reflection matrix $\mathbf{r}_{L,T}$ with the incoming wave $\mathbf{E}=(E_x,E_y)$

$$\mathbf{E}'=\mathbf{r}_{L,T}\mathbf{E}. \tag{1}$$

For *x* perpendicular and *y* parallel to the reflection plane $\mathbf{r}_{L,T}$ take simple forms. For L-MOKE $\mathbf{r}_L$ adopts the form[35–37]

$$r_L=\begin{pmatrix} r_{ss} & \pm\Delta_{sp} \\ \mp\Delta_{sp} & r_{pp} \end{pmatrix}. \tag{2}$$

For T-MOKE $\mathbf{r}_T$ has the form

$$\mathbf{r}_T=\begin{pmatrix} \mathbf{r}_{ss} & 0 \\ 0 & r_{pp}\pm\Delta_{pp} \end{pmatrix}. \tag{3}$$

The terms $|r_{ss}|^2$ and $|r_{pp}|^2$ are identical to the nonmagnetic Fresnel reflectances R_s and R_p, respectively. The indices *s* (*p*) indicate the experimental geometry, i.e., whether the polarization plane of the incident linearly polarized light is perpendicular (parallel) to the reflectivity plane, see the schematic set-up shown in Fig. 1. The magnetic contribution to the reflectivity is comprised by Δ_{sp} and Δ_{pp} where the signs $\pm$ refer to the two antiparallel magnetization directions.

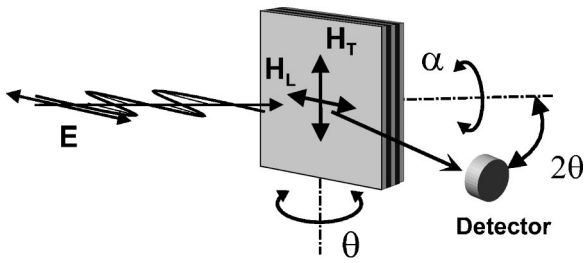

FIG. 1. Schematic set-up for reflectivity experiments on samples with variable longitudinal magnetic field H_L (L-MOKE) and transversal field H_T (T-MOKE) applied in the surface plane. The angle of grazing incidence θ can be set between 0° and 85°, the detector can be moved independently by 2θ in the plane of reflectance and both are rotatable around the azimuth α. T-MOKE is observed when linearly polarized light with electric-field vector *E* in the plane of incidence (*p* geometry, $\alpha=90°$) is reflected off a sample with field H_T.

Once these coefficients are known, every x-ray reflectivity experiment can completely be described. The reflected intensity is given by

$$I'_{\pm}=(|E'_x|^2+|E'_y|^2). \tag{4}$$

We describe the polarization of the incident light by the normalized Stokes parameters S_1, S_2, S_3 (Refs. 38, 39) as

$$\begin{aligned} S_1&=(|E_x|^2-|E_y|^2)/I_0, \\ S_2&=(E_xE_y^*+E_x^*E_y)/I_0, \\ S_3&=(E_xE_y^*-E_x^*E_y)/I_0, \end{aligned} \tag{5}$$

where $I_0=(|E_x|^2+|E_y|^2)$ is the incident intensity. The components S_1 and S_2 give the degree of linear polarization in (*x*-*k*) plane and the degree of linear polarization in the plane diagonal to (*x*-*k*) and (*y*-*k*) plane, respectively. S_3 stands for the degree of circular polarization. Our experimental set-up is chosen such that $S_2=0$ and we assume fully polarized light, which is valid for our experiment.[25] In the T-MOKE geometry the absolute reflectance is

$$\begin{aligned} R_{T\pm}=I_{T\pm}/I_0&=(\tfrac{1}{2}|r_{ss}|^2+\tfrac{1}{2}|r_{pp}\pm\Delta_{pp}|^2) \\ &+S_1\cos(2\alpha)(\tfrac{1}{2}|r_{ss}|^2-\tfrac{1}{2}|r_{pp}\pm\Delta_{pp}|^2). \end{aligned} \tag{6}$$

For L-MOKE we obtain

$$\begin{aligned} R_{L\pm}=I_{L\pm}/I_0&=(\tfrac{1}{2}|r_{ss}|^2+\tfrac{1}{2}|r_{pp}|^2+|\Delta_{sp}|^2) \\ &+S_1\cos(2\alpha)(\tfrac{1}{2}|r_{ss}|^2-\tfrac{1}{2}|r_{pp}|^2)\pm S_1\sin(2\alpha) \\ &\times[\mathrm{Re}\{-\Delta_{sp}^*(r_{ss}-r_{pp})\}]\pm S_3\,\mathrm{Im}\{-\Delta_{sp}^*(r_{ss}+r_{pp})\}. \end{aligned} \tag{7}$$

These are general equations for any reflection geometry which is determined by the azimuthal angle α. Here we treat the special case $\alpha=0°$ and 90°, which correspond to the *s* and *p* geometry, respectively. For a demagnetized sample we have $\Delta_{pp}=0$ and $\Delta_{sp}=0$. For the investigation of reflection

coefficients of each individual layer in a multilayer system, this formalism has to be extended and interference effects have to be taken into account.[9,17,33,34] In this paper we treat the multilayer system as an uniform sample with effective reflection coefficients. The individual terms of Eqs. (6) and (7) are experimentally accessible according to Eqs. (8)–(13) by the indicated magnetization and reflectivity geometry:

$$|r_{pp}|^2 = R_p, \quad \text{nonmagnetic}, \quad S_1 = 1, \quad \text{p geometry}, \tag{8}$$

$$|r_{ss}|^2 = R_s, \quad \text{nonmagnetic}, \quad S_1 = 1, \quad \text{s geometry}, \tag{9}$$

$$|\Delta_{pp}|^2 = \tfrac{1}{2}(R_{T+} + R_{T-}) - |r_{pp}|^2, \quad \text{transversal}, \quad S_1 = 1, \quad \text{p geometry}, \tag{10}$$

$$|\Delta_{sp}|^2 = \tfrac{1}{2}(R_{L+} + R_{L-}) - |r_{pp}|^2, \quad \text{longitudinal}, \quad S_1 = 1, \quad \text{p geometry}, \tag{11}$$

$$\mathrm{Re}\{\Delta_{pp}^* r_{pp}\} = \tfrac{1}{4}(R_{T+} - R_{T-}), \quad \text{transversal}, \quad S_1 = 1, \quad \text{p geometry}, \tag{12}$$

$$\mathrm{Im}\{-\Delta_{sp}^*(r_{ss} + r_{pp})\} = \tfrac{1}{2}(R_{L+} - R_{L-}), \quad \text{longitudinal}, \quad S_3 = 1, \quad \text{p geometry}. \tag{13}$$

The coefficients are directly related to the optical constants of the material and are discussed partly in Ref. 37. For the case of circularly polarized light, Eq. (13) can be expressed in terms of the magneto-optical refractive index $n_\pm$

$$n_\pm = 1 - (\delta_0 \pm \Delta\delta) + i(\beta_0 \pm \Delta\beta), \tag{14}$$

where the charge contributions (δ_0, β_0) and magnetic contributions $(\Delta\delta, \Delta\beta)$ are separated in both, the refractive and the absorptive part. According to Ref. 37 we obtain

$$\mathrm{Im}\{-\Delta_{sp}^*(r_{ss} + r_{pp})\} = \Delta\delta \frac{4\bar{n}(\sin^2\theta - \sin^2\theta_t)\sin\theta}{[(\bar{n}^2+1)\cos(\theta+\theta_t) + 2\bar{n}]^2 \sin\theta_t} \tag{15}$$

with the average $\bar{n} = \frac{1}{2}(n_+ + n_-)$ and the angle of incidence θ and the angle of refraction θ_t, both measured relative to the surface. The relation between $\mathrm{Im}\{-\Delta_{sp}^*(r_{ss}+r_{pp})\}$ and the magnetic contribution $\Delta\delta$ is expressed by Eq. (15). The relation between the optical constants and $\mathrm{Re}\{\Delta_{pp}^* r_{pp}\}$ [Eq. (12)] is more complex and is not closer examined.

B. Asymmetry

Even without the knowledge of the *absolute reflection* coefficients information about the magnetic contribution to the reflectance can be obtained by the measurements of the reflected intensities upon reversal of the magnetic field. From these the asymmetry parameters A_T and A_L, as defined in the introduction, are deduced. For T-MOKE we find from Eq. (6) for p geometry

$$A_T = a_T(1 + S_1)/(1 - p_T S_1), \tag{16}$$

$$\text{with} \quad a_T = 2\,\mathrm{Re}\{\Delta_{pp}^* r_{pp}\}/[|r_{ss}|^2 + |r_{pp}|^2 + |\Delta_{pp}|^2],$$

$$\text{and} \quad p_T = (|r_{ss}|^2 - |r_{pp}|^2 - |\Delta_{pp}|^2)/(|r_{ss}|^2 + |r_{pp}|^2 + |\Delta_{pp}|^2).$$

In the L-MOKE geometry with $\alpha = 90°$, we obtain for the asymmetry parameter A_L [see Eq. (7)]

$$A_L = (a_L S_3)/[1 - p_L(1 - S_3^2)^{1/2}], \tag{17}$$

$$\text{with} \quad a_L = 2\,\mathrm{Im}\{-\Delta_{sp}^*(r_{ss} + r_{pp})\}/(|r_{ss}|^2 + |r_{pp}|^2 + 2|\Delta_{sp}|^2),$$

$$\text{and} \quad p_L = (|r_{ss}|^2 - |r_{pp}|^2)/(|r_{ss}|^2 + |r_{pp}|^2 + 2|\Delta_{sp}|^2).$$

These equations show that the measured asymmetry parameters A_T, A_L can be split into two contributions, the magnetic asymmetry a_T (a_L) almost proportional to the magnetization and the polarizing power of the sample p_T (p_L) almost independent of the magnetization. The polarizing power strongly depends on the angle of incidence, in particular, close to the Brewster angle near 45° it can reach a maximum close to 1, since $|r_{pp}|^2$ is close to zero. At small incident angles, which is generally the case when using hard x rays, this influence is negligible, and therefore the measured asymmetries are linear in S_1 and S_3, respectively. For soft x rays the polarizing power of a reflection sample cannot be neglected as Eqs. (16) and (17) show, an effect that has not to be taken into account for transmission experiments. Depending on the size of p_T (p_L), the measured asymmetry parameters A_T (A_L) are not linear in the polarization S_1 (S_3). The strongest deviations of $A_T(S_1)$ from the linear behavior occurs for $p_T = 1$. However, the relation $A_T < 1$ is always fulfilled as is obvious from its definition.[31,40] Furthermore in T-MOKE the asymmetry can also be measured with $S_1 = 0$, i.e., unpolarized light, while in L-MOKE experiments the asymmetry is zero when $S_3 = 0$.

In summary, Eqs. (16) and (17) show that the measured asymmetry strongly depends on the interplay between the polarization of the incident light and the polarizing power of the sample. Thus the experimental geometry is essential in the soft x-ray range. Note that the nonlinearity of the asymmetry enters by normalizing the difference signal to the sum of the reflected intensities. In contrast, a linear dependence of the magnetic contribution to the reflectance on the degree of the respective Stokes parameter is observed if the absolute reflectance is measured [see Eqs. (6) and (7)].

III. EXPERIMENT

The experiment was performed at BESSY II using the elliptical undulator beamline UE56/1-PGM.[25] The spectral resolution at the Fe-2p edge was $E/\Delta E = 2500$ and the polarization was tunable from fully linear $(S_1 = 1)$ to circular $(S_3 = 0.96)$ with an accuracy and reproducibility better than 2%.[25] The polycrystalline Fe/C multilayer (period $d = 3.11$ nm $d_{\mathrm{Fe}} = 2.56$ nm, $d_C = 0.55$ nm, $P = 100$ periods) was magnetron-sputter deposited[41,42] on a Si wafer and capped with a 2.5-nm-Al layer. The depth profile of the oxidation state of the Fe-top layers was determined by x-ray

photo emission spectroscopy (XPS), using an Al-K-alpha source, after sputtering the sample surface. The data showed a 1.9 ± 0.1-nm oxidized Al-cap layer. The oxidation degree of the uppermost Fe layer is $25\%\pm5\%$. The following Fe layers are less than 2% oxidized. A multilayer was preferred over a simple Fe layer to obtain a sufficient reflectivity even at large angles of incidence. The experiments (see Fig. 1) were done with the BESSY polarimeter.[43] *In situ* exchange and removal of samples allowed for quasisimultaneous detection of the incident and the reflected light in order to measure the absolute reflectance. Two magnetic-coil systems supplied variable fields between ±500 Oe in the sample plane parallel (L-MOKE) or perpendicular (T-MOKE) to the plane of incidence. The angle of incidence could be tuned from $\theta=0°$ (grazing incidence) to 85° (near normal incidence) while the GaAsP photodiode that is insensitive to the polarization state of light moved by 2θ to monitor the reflected beam. Additionally, the detector together with the sample could be moved around the azimuth α which allowed to set s-($\alpha=0°$), p-($\alpha=90°$) or any intermediate geometry. All measurements were performed with saturated ferromagnetic samples or, where indicated, with demagnetized samples. The latter were achieved by an oscillating coil current with decreasing amplitude.

IV. RESULTS AND DISCUSSION

A. T-MOKE

The reflectance spectra $R_{T\pm}$ of linearly polarized light across the Fe-$2p$ edge are shown in the top panel of Fig. 2. The reflectance is resonantly enhanced when exciting the spin-orbit split Fe-$2p_{3/2}$ and $2p_{1/2}$ states. At these energies strong changes in the reflectance occur upon reversal of the magnetic field. The corresponding asymmetry A_T reaches values of up to 40% near the Fe $2p_{3/2}$ edge (Fig. 2, middle part) which are larger than those observed in absorption experiments.[2,24,25] Near the Fe-$2p_{3/2}$ edge the Fe/C multilayer shows strong modulations of the reflectivity. These can be explained by interference effects, i.e., Kiessig fringes of the Bragg reflectivity which are resonantly enhanced close to an absorption edge. In addition the partially oxidized Fe-top layer has to be taken into account which leads to additional spectral structures.[23] The relative influence of the oxidized top-Fe layer depends on the angle of incidence and the photon energy. Taking into account the absorption length of 30 nm at the Fe-$2p_{3/2}$ edge the partially oxidized and additional two nonoxidized Fe layers contribute to the reflecting process at $\theta=18°$. For the discussion of the polarization dependence of magnetic reflectivity in this paper, these modulations are of no direct relevance. We have discussed those in detail in Ref. 40, 42.

We systematically recorded such reflectivity and asymmetry spectra for different degrees of linear polarization S_1. The deduced asymmetry parameters A_T were evaluated at several energies and plotted as a function of S_1 in Fig. 2 (bottom, symbols). The data are fitted according to Eq. (16) (lines) with fit parameters a_T and p_T. As expected from Eq. (16) we observe a nonvanishing asymmetry at $S_1=0$, where the measured asymmetry A_T is identical to the magnetic

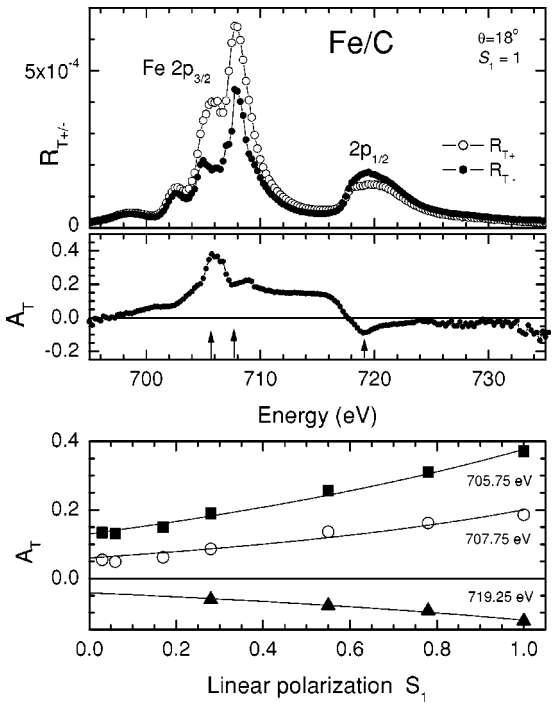

FIG. 2. Top, the reflectances R_{T+} and R_{T-} of linearly polarized soft x rays measured from a Fe/C multilayer across the Fe-$2p$ edge. Middle: the corresponding asymmetry A_T. Bottom: the asymmetry A_T as a function of S_1 (symbols), deduced from spectra like those shown above, at various indicated energies (see arrows). The solid lines show a fit of the data using Eq. (16). A nonvanishing asymmetry is observed at $S_1=0$. The error bars are smaller than the symbol size.

asymmetry a_T. This shows that the magnetic response can be obtained even with circularly or nonpolarized light as mentioned above. The explanation of this is the simple fact that circularly or even unpolarized light always contains an electric-field component E, parallel to the plane of incidence, which is relevant for T-MOKE experiments.

The reflectance $R_{T\pm}$ of linearly polarized light as a function of the angle of incidence for one fixed photon energy at the Fe-$2p_{3/2}$ edge are plotted in Fig. 3 (top). As expected, the reflectance decreases with increasing angle of incidence. It is enhanced at the Bragg peaks that appear in first, second, and third order near $\theta=16°$, 34°, and 57°, respectively. The asymmetry parameter A_T (Fig. 3, middle) is negligible at grazing incidence ($\theta\leqslant4°$), where the penetration depth of the light perpendicular to the sample surface is small, and the reflectance is dominated by the nonmagnetic Al-cap layer. In this region no magnetic information from Fe is obtained. With the angle of incidence, the penetration depth of the light and thus the number of reflecting layers increases. Up to nine Fe layers contribute to the reflection process at $\theta=65°$, taking into account the absorption length of 30 nm at the Fe-$2p_{3/2}$ edge.

The asymmetry reaches up to 70% and shows strong modulations and even a sign reversal. These modulations are explained by the interference effects of optical reflections from a multilayer structure and the movement of standing waves across the interfaces between magnetic Fe and the

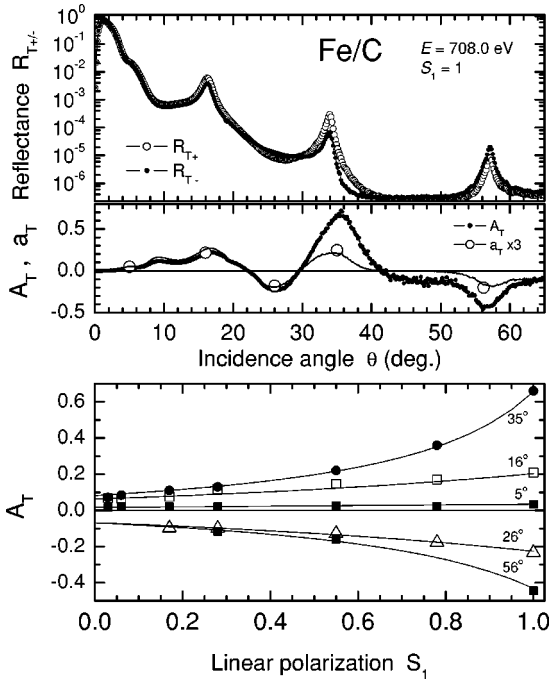

FIG. 3. Top: the reflectances R_{T+} and R_{T-} of linearly polarized light as a function of the angle of incidence for a fixed photon energy at the Fe-$2p_{3/2}$ edge. Middle panel, the measured asymmetry A_T (points). Open circles, the magnetic asymmetry a_T obtained from a fit of Eq. (16) to the data shown in the bottom panel. Line, recalculation of a_T from the measured A_T using the theoretical data for p_T taken from Fig. 4. Note that a_T is multiplied by a factor of 3. Bottom, the measured asymmetry A_T as a function of the incident linear polarization S_1 for various incident angles. The curves shown were fitted according to Eq. (16) with p_T and a_T as fit parameters. Note that the asymmetry A_T is nonlinear in the polarization and nonvanishing at $S_1=0$. Error bars are smaller than the symbol size.

nonmagnetic C layers.[40,42] This effect is well known and has been utilized to probe the magnetic depth profile of layered magnetic systems. In particular, the standing wave technique provides insight into the magnetic properties at interfaces as magnetic dead layers or the modification of the magnetism due to intermixing effects.[21,44] However, such investigations are not the topic of this paper. Here we concentrate on the polarization dependence of the reflectivity experiments, treating the multilayer as an uniform sample, not resolving the individual layers.

Reflectivity spectra as shown in Fig. 3 (top) were systematically recorded for different degrees of linear polarization S_1 in order to examine the asymmetry parameters A_T as a function of S_1. The results are plotted in Fig. 3 (bottom) for several angles of incidence together with the fit according to Eq. (16) (lines). The magnetic asymmetry a_T and the polarizing power p_T determined by the fit are shown as open circles in the middle panel of Fig. 3 and bold circles in Fig. 4, respectively. For $S_1=0$, the asymmetry does not vanish, in agreement with the findings presented in Fig. 2 (bottom). The asymmetry increases linearly with S_1 for small angles of incidence ($\theta<26°$) while for larger angles significant deviations from linearity occur. More insight in this functional dependence can be obtained from analyzing the influence of

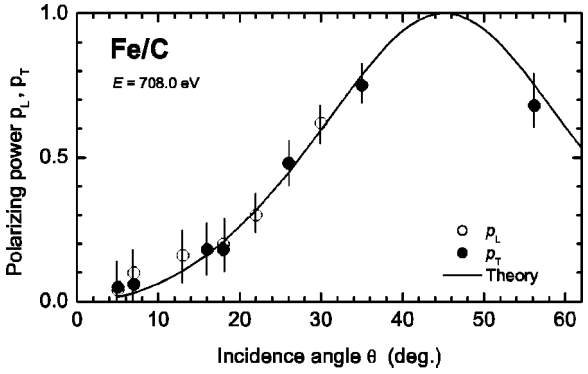

FIG. 4. The polarizing powers p_T and p_L obtained from fits with Eqs. (16) and (17) to the data in Figs. 3 and 6 (bottom), respectively. The curve is calculated from nonmagnetic reflectivity data based on the Henke table, neglecting Δ_{pp} and Δ_{sp}. The polarizing power reaches its maximum at the Brewster angle at 45°.

the polarizing power p_T on the measured asymmetry. The magnetic asymmetry a_T that results from a fit to the data $A_T(S_1)$ is close to the measured asymmetry A_T for small angles of incidence (Fig. 3 middle, open circles), but with increasing angle, a_T significantly deviates from A_T. Note that the data a_T are multiplied by a factor of three. The difference between a_T and A_T is fully understood: it results from the term $p_T S_1$ [denominator in Eq. (16)] which is dominated by the polarizing power p_T. It increases with the angle of incidence as shown in Fig. 4. The experimental data for p_T agree well with the calculations (Fig. 4, line) for the Fe/C multilayer, based on the Fresnel equations. The optical constants used for C and nonmagnetic Fe, neglecting Δ_{pp} and Δ_{sp} were taken from the Henke table.[45] The maximum of p_T and thus the strongest deviation of $A_T(S_1)$ from linear behavior is expected at the Brewster angle around 45°. In turn, the knowledge of this general curve $p_T(\theta)$ allows one to deduce a_T from the measured A_T according to Eq. (16) for any angle of incidence. The recalculated data a_T (Fig. 3, center, line) agree well with those obtained from the fit. This angle-dependent difference between a_T and A_T shows that for the quantitative analysis of T-MOKE experiments the knowledge of the polarizing power of the sample under investigation is essential.

B. L-MOKE

The reflectance spectra $R_{L\pm}$ of circularly polarized light across the Fe-$2p$ edge are shown in the top panel of Fig. 5. Also in this geometry pronounced changes in the reflectance occur upon the reversal of the magnetic field. The corresponding asymmetry A_L reaches values of up to 35% near the Fe-$2p_{3/2}$ edge (Fig. 5, bottom panel) which are again larger than those obtained from absorption experiments.[1,2,24,25] The modulations close to the $2p_{3/2}$ edge are explained in the same manner as those observed for T-MOKE.

The reflectance $R_{L\pm}$ of circularly polarized light as a function of the angle of incidence for fixed photon energy at the Fe-$2p_{3/2}$ edge are plotted in Fig. 6 (top). Similar to the

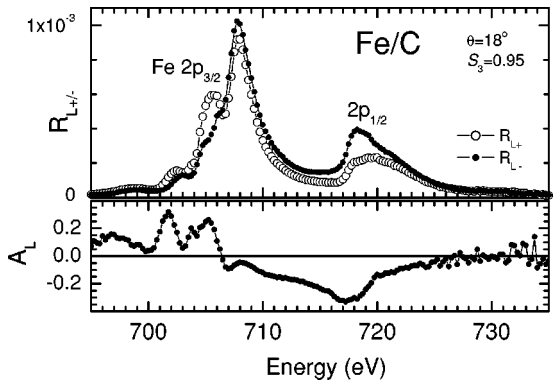

FIG. 5. Top, reflectances R_{L+} and R_{L-} of circularly polarized soft x rays from a longitudinally magnetized Fe/C multilayer across the Fe-$2p$ edge. Bottom, corresponding measured asymmetry A_L.

T-MOKE experiments (Fig. 3) the reflectance decreases with increasing angle of incidence showing Bragg peaks in first and second order. The asymmetry shows strong modulations with the angle of incidence, similar to the findings for T-MOKE. In L-MOKE sharp resonances appear additionally in A_L at the Bragg angles around 16° and 34°. These features result from the strong magnetization dependence of the refractive part of the optical constants resulting in a change of the Bragg peak position and width depending on the magnetization. This in turn can be exploited to determine the complete set of magneto-optical constants across an absorption edge.[46,47]

The polarization dependence of the asymmetry A_L is plotted in Fig. 6 (bottom) for several angles of incidence (symbols) together with the fit result according to Eq. (17) (lines). The magnetic asymmetry a_L and the polarizing power p_L determined by the fit are shown as open circles in the middle panel of Fig. 6 and in Fig. 4, respectively. As expected from Eq. (17) the asymmetry in L-MOKE is zero for $S_3=0$ and increases with increasing degree of circular polarization giving $A_L=a_L$ for $S_3=1$. For angles $\theta<22°$ an almost linear dependence is observed while for larger angles deviations from linearity occur. The deviation from linearity is not due to the saturation effects but due to the influence of the polarizing power p_L of the sample which enters the denominator of Eq. (17). As we find from T-MOKE experiments, the polarizing power increases with increasing angle (Fig. 4) and it agrees with calculations (line) for the Fe/C multilayer. This influence of p_L can lead to larger values of the measured A_L for elliptical than for circularly polarized light. For example, the data taken at 30° have a maximum around $S_3=0.75$ and decrease towards $S_3=1$, an anomaly that was already noted by Kao *et al.*[16]. A similar dependence of the asymmetry at different angles of incidence was recently found at the $2p$ edge of Fe and the $3d$ edge of Gd for Gd/Fe multilayers[48,49]. In contrast to T-MOKE experiments, the magnetic asymmetry a_L (open circles) as deduced from the fit to the curve $A_L(S_3)$ is close to the measured asymmetry A_L for all angles of incidence (Fig. 6, center). Only for larger angles they slightly deviate due to the increasing influence of p_L. A recalculation of a_L (line), using the theoretical curve $p_L(\theta)$ (Fig. 4) again shows the close relationship to the measured

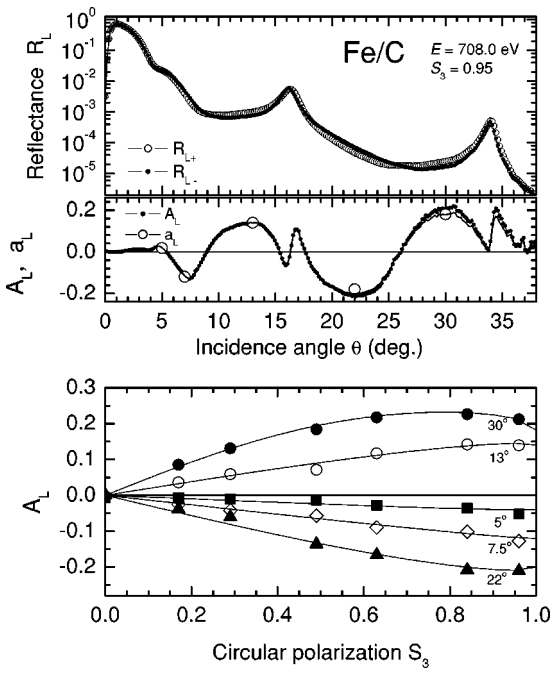

FIG. 6. Top, the reflectances R_{L+} and R_{L-} of circularly polarized light as a function of the angle of incidence for fixed photon energy at the Fe-$2p_{3/2}$ edge. Center, the measured asymmetry A_L (points). Open circles, magnetic asymmetry a_L obtained from a fit using Eq. (17) to the data shown in the bottom panel. Line, recalculation of a_L from the measured A_L using the theoretical data for p_L taken from Fig. 4. Bottom, the measured asymmetry A_L as a function of the incident circular polarization S_3 for various incident angles. The curves shown are fits of the data points according to Eq. (17) with p_L and a_L as fit parameters. Error bars are smaller than the symbol size.

asymmetry A_L. Thus, for the quantitative analysis of intensity measurements in the L-MOKE geometry the knowledge of the polarizing power of the sample under investigation is less crucial than for the T-MOKE geometry.

V. REFLECTION COEFFICIENTS

A summary of the individual coefficients of the reflection matrix for our Fe/C sample is given in Fig. 7, determined from the experimental data according to Eqs. (8)–(13). The absolute values of the nonmagnetic parts R_s and R_p are obtained from measurements of the demagnetized sample with linearly polarized light in s or p geometry, respectively, [Fig. 7(a)]. As mentioned in Sec. IV the modulations in R_s and R_p close to the Fe-$2p_{3/2}$ edge can be attributed to interference effects and to partially oxidized Fe.

With the knowledge of R_p the absolute value of the magnetic contribution $|\Delta_{pp}|^2$ is obtained as the difference spectrum to the average of the T-MOKE spectra R_{T+} and R_{T-} [Eq. (10)]. The result is shown in Fig. 7(b). The magnetic contribution $|\Delta_{sp}|^2$ is determined as the difference between the spectrum R_p and the average of the L-MOKE spectra R_{L+} and R_{L-} [Eq. (11)]. The result is shown in Fig. 7(c). Note that both spectra $|\Delta_{pp}|^2$ and $|\Delta_{sp}|^2$ can be determined with linearly polarized light in p geometry and without the

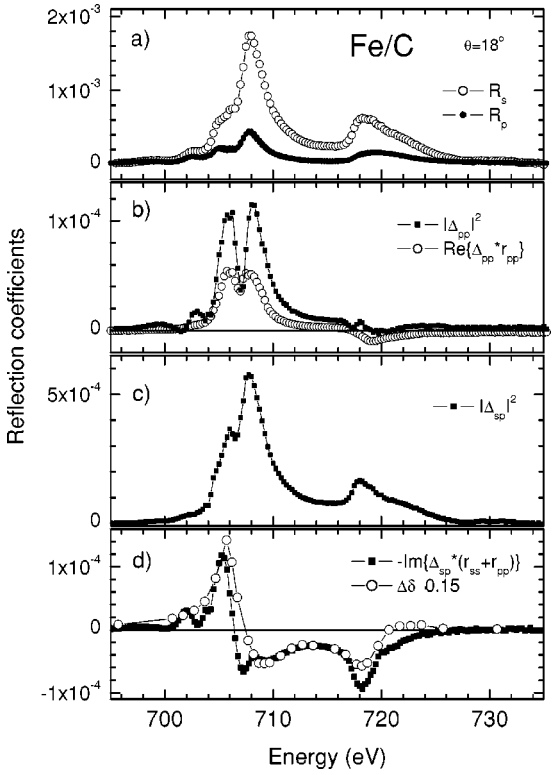

FIG. 7. Spectral dependence of the various individual coefficients of the reflectance matrix [see Eqs. (2) and (3)] as determined from the experimental data using Eqs. (8)–(13). (a) The nonmagnetic reflectance coefficients R_s and R_p [Eqs. (8) and (9)]. (b) The magnetic coefficients for a transversal field [Eqs. (10) and (12)]. (c) The absolute value of the magnetic coefficient for a longitudinal field [Eq. (11)]. (d) The magnetic coefficients for a longitudinal field [Eq. (13)]. The magnetic contribution $\Delta\delta$ of the optical constant $n_\pm$ was obtained independently from Bragg scattering and, additionally, from Faraday measurements on an identical sample.[47] In accordance with Eq. (15) the latter curve was scaled by a factor of 0.15.

knowledge of R_s, because the latter cancels due to averaging of $R_{T\pm}$ and $R_{L\pm}$, respectively.

The cross terms of the magnetic and nonmagnetic contributions to the reflection matrix are obtained from the T- and L-MOKE difference spectra $(R_{T+}-R_{T-})$ and $(R_{L+}-R_{L-})$, respectively. The data are shown in Figs. 7(b) and 7(d). The difference spectra of the absolute reflectance directly give the magnetic information, while the corresponding asymmetry spectra A_T and A_L (Figs. 2 and 5) are influenced by the polarizing power of the sample. The enlarged structures in A_T and A_L away from the $2p$ edge arise due to the influence of the normalization with respect to the average reflectance which is close to zero.

In L-MOKE the cross term $\mathrm{Im}\{-\Delta_{sp}^*(r_{ss}+r_{pp})\}$ can be related to the optical constant $n_\pm$ for circularly polarized light according to Eq. (15). As expected, we find a close relationship to the magnetic contribution $\Delta\delta$ [Fig. 7(d)]. The spectrum $\Delta\delta$ was obtained independently by resonant magnetic Bragg scattering of circularly polarized soft x rays on the same sample.[47] These experimental data are confirmed by a Faraday measurement on an identical, simultaneously grown sample, but measured in transmission.[47] Differences between $\mathrm{Im}\{-\Delta_{sp}^*(r_{ss}+r_{pp})\}$ and $\Delta\delta$ may be explained by the energy dependence of the term containing the refractive angle θ_t [see Eq. (15)] and by the non-negligible interference effects of the multilayer sample.

VI. CONCLUSION

Resonant magnetic reflectivity experiments of polarized soft x rays across the Fe-$2p$ absorption edge on a ferromagnetic Fe/C multilayer have been performed in the longitudinal (L-MOKE) and the transversal (T-MOKE) geometry. The reflectance as a function of the degree of polarization can be described in a framework that is based on the reflection matrix and the Stokes formalism. The T- and L-MOKE asymmetry parameters which were analyzed as a function of the respective Stokes parameters, show a nonlinear dependence for larger angles of incidence. This behavior is well explained within our formalism for any photon energy or angle of incidence. The reason for this nonlinearity is the polarizing power of the reflecting sample which enters through the normalization of the T- or L-MOKE asymmetry spectra. The knowledge of the polarizing power in turn allows for a rescaling of the measured data and thus the determination of the magnetic asymmetry parameter. The absolute values of the nonmagnetic and magnetic terms of the reflection matrix are completely determined from reflectance spectra across the Fe-$2p$ edge. In L-MOKE, the magnetic reflection coefficients can be attributed to the magnetic contributions to the optical constant. To this end a direct determination of both the real and imaginary parts of the optical constants by reflectivity measurements is not possible. For a separate determination of the real and imaginary parts of the reflection coefficients, a measurement of the phase in addition to the intensity is necessary. This requires a polarization analysis of the reflected light.

ACKNOWLEDGMENTS

We thank B. Schnyder for doing the XPS depth profile of the sample. This project was supported by the European Community (Grant No. ERBFMGECT980105), the Swiss Federal Office for Education and Science (Grant No. BBW97.0392) and the German Federal Ministery for Education and Science (BMBF, Grant No. 05KS1IPB/8).

*Corresponding author: H.-Ch. Mertins, BESSY, Albert-Einstein-Strasse 15, D-12489 Berlin, Germany. Fax: 49-30-6392-4980. Email address: mertins@bessy.de

[1] C. T. Chen, Y. U. Idzerda, H.-J. Lin, N. V. Smith, G. Meigs, E. Chaban, G. H. Ho, E. Pellegrin, and F. Sette, Phys. Rev. Lett. **75**, 152 (1995).

[2] J. B. Kortright, D. D. Awschalom, J. Stöhr, S. D. Bader, Y. U. Idzerda, S. S. P. Parkin, I. K. Schuller, and H.-C. Siegmann, J.

Magn. Magn. Mater. **207**, 7 (1999).
[3] J. B. Kortright, M. Rice, and R. Carr, Phys. Rev. B **51**, 10 240 (1995).
[4] H.-Ch. Mertins, F. Schäfers, X. Le Cann, A. Gaupp, and W. Gudat, Phys. Rev. B **61**, R874 (2000).
[5] J. Kunes, P. M. Oppeneer, H.-Ch. Mertins, F. Schäfers, A. Gaupp, W. Gudat, and P. Novak, Phys. Rev. B **64**, 174417 (2001).
[6] D. Knabben, N. Weber, B. U. Raab, Th. Knoop, F. U. Hillebrecht, E. Kisker, and G. Y. Guo, J. Magn. Magn. Mater. **190**, 349 (1998).
[7] S. S. Dhesi, G. van der Laan, E. Dudzik, and A. B. Shick, Phys. Rev. Lett. **87**, 077201 (2001).
[8] H.-Ch. Mertins, P. M. Oppeneer, J. Kunes, A. Gaupp, D. Abramsohn, and F. Schäfers, Phys. Rev. Lett. **87**, 047401 (2001).
[9] J. B. Kortright and S. K. Kim, Phys. Rev. B **62**, 12 216 (2000).
[10] H. A. Dürr, E. Dudzik, S. S. Dhesi, J. B. Goedkoop, G. van der Laan, M. Belakhovsky, C. Moduta, A. Marty, and Y. Samson, Science **284**, 2166 (1999).
[11] P. Fischer, T. Eimüller, G. Schütz, G. Schmahl, P. Guttmann, and G. Bayreuther, J. Magn. Magn. Mater. **198-199**, 624 (1999).
[12] F. U. Hillebrecht, H. Ohldag, N. B. Weber, C. Bethke, U. Mick, M. Weiss, and J. Bahrdt, Phys. Rev. Lett. **86**, 3419 (2001).
[13] F. Nolting, A. Scholl, J. Stöhr, J. W. Seo, J. Fompeyrine, H. Siegwart, J.-P. Locquet, S. Anders, J. Lüning, E. E. Fullerton, M. F. Toney, M. R. Scheinfein, and H. A. Padmore, Nature (London) **405**, 767 (2000).
[14] W. Kuch, X. Gao, and J. Kirschner, Phys. Rev. B **65**, 064406 (2002).
[15] G. A. Prinz, Science **282**, 1660 (1998).
[16] C. C. Kao, C. T. Chen, E. D. Johnson, J. B. Hastings, H. J. Lin, G. H. Ho, G. Meigs, J.-M. Brot, S. L. Hulbert, Y. U. Idzerda, and C. Vettier, Phys. Rev. B **50**, 9599 (1994).
[17] J. Geissler, E. Goering, M. Justen, F. Weigand, G. Schütz, J. Langer, D. Schmitz, H. Maletta, and R. Mattheis, Phys. Rev. B **65**, 020405 (2001).
[18] M. Sacchi and A. Mirone, Phys. Rev. B **57**, 8408 (1998).
[19] A. Dechelette, J. M. Tonnerre, M. C. Saint Lager, F. Bartolome, L. Seve, D. Raoux, H. Fischer, M. Piecuch, V. Chakarian, and C. C. Kao, Phys. Rev. B **60**, 6636 (1999).
[20] L. Seve, N. Jaouen, J. M. Tonnerre, D. Raux, F. Bartolome, M. Arend, W. Felsch, A. Rogalev, J. Goulon, C. Gautier, and J. F. Berar, Phys. Rev. B **60**, 9662 (1999).
[21] S. K. Kim and J. B. Kortright, Phys. Rev. Lett. **86**, 1347 (2001).
[22] S. W. Lovesey and S. P. Collins, *X-ray Scattering and Absorption by Magnetic Materials* (Clarendon Press, Oxford, 1996).
[23] H.-J. Kim, J.-H. Park, and E. Vescovo, Phys. Rev. B **61**, 15 284 (2000).
[24] K. Holldack, F. Schäfers, T. Kachel, and I. Packe, Rev. Sci. Instrum. **67**, 2485 (1996).
[25] M. R. Weiss, R. Follath, K. J. S. Sahwney, F. Senf, J. Bahrdt, W. Frentrup, A. Gaupp, S. Sasaki, M. Scheer, H.-Ch. Mertins, D. Abramsohn, F. Schäfers, W. Kuch, and W. Mahler, Nucl. Instrum. Methods Phys. Res. A **467-8**, 449 (2001).
[26] H. Hochst, D. Zhao, and D. L. Huber, in *Magnetic Ultrathin Films, Multilayers and Surfaces—1997*, edited by J. Tobin, D. Chambliss, D. Kubinski, K. Barmak, P. Dederichs, W. de Jonge, T. Katayama, and A. Schuhl, MRS Symposia Proceedings No. 475 (Materials Research Society, Pittsburgh, 1997), p. 315.
[27] J. P. Hannon, G. T. Trammell, M. Blume, and D. Gibbs, Phys. Rev. Lett. **61**, 1245 (1988).
[28] M. Blume and D. Gibbs, Phys. Rev. B **37**, 1779 (1988).
[29] P. M. Brunel, G. Patrat, F. de Bergevin, F. Rousseaux, and M. Lemmonier, Acta Crystallogr., Sect. A: Found. Crystallogr. **A39**, 84 (1983).
[30] J. P. Hill and D. F. McMorrow, Acta Crystallogr., Sect. A: Found. Crystallogr. **A52**, 236 (1996).
[31] F. de Bergevin, M. Brunel, R. M. Galera, C. Vettier, E. Elkaim, M. Bessiere, and S. Lefebvre, Phys. Rev. B **46**, 10 772 (1992).
[32] J. M. Tonnerre, in *Magnetism and Synchrotron Radiation*, edited by E. Beaurepaire, B. Carriere, and J.P. Kappler (Les Editions de Physique, Paris, 1997), p. 245.
[33] J. Zak, E. R. Moog, C. Liu, and S. D. Bader, Phys. Rev. B **43**, 6423 (1991).
[34] S. A. Stepanov and S. K. Sinha, Phys. Rev. B **61**, 15 302 (2000).
[35] M. J. Freiser, IEEE Trans. Magn. **MAG-4**, 152 (1967).
[36] Z. J. Yang and M. R. Scheinfein, J. Appl. Phys. **74**, 6810 (1993).
[37] P. M. Oppeneer, in *Handbook of Magnetic Materials*, edited by K. H. J. Buschow (Elsevier, Amsterdam, 2001), Vol. 13, pp. 229–422.
[38] W. B. Westerveld, K. Becker, P. W. Zetner, J. J. Corr, and J. W. McConkey, Appl. Opt. **24**, 2256 (1985).
[39] M. Born and E. Wolf, *Principles of Optics* (Pergamon Press, Oxford, 1980).
[40] H.-Ch. Mertins, O. Zaharko, F. Schäfers, A. Gaupp, D. Abramsohn, M. Weiss, and H. Grimmer, Nucl. Instrum. Methods Phys. Res. A **467-8**, 1415 (2001).
[41] H. Grimmer, O. Zaharko, M. Horisberger, H.-Ch. Mertins, F. Schäfers, and U. Staub, Proc. SPIE **3773**, 224 (1999).
[42] O. Zaharko, H.-Ch. Mertins, H. Grimmer, and F. Schäfers, Nucl. Instrum. Methods Phys. Res. A **467-8**, 1419 (2001).
[43] F. Schäfers, H.-Ch. Mertins, A. Gaupp, W. Gudat, M. Mertin, I. Packe, F. Schmolla, S. Di Fonzo, G. Soullié, W. Jark, R. Walker, X. Le Cann, M. Eriksson, and R. Nyholm, Appl. Opt. **38**, 4074 (1999).
[44] S. K. Kim, J. R. Jeong, J. B. Kortright, and S. C. Shin, Phys. Rev. B **64**, 052406 (2001).
[45] B. L. Henke, E. Gullikson, and J. C. Davis, http://www-cxro.lbl.gov/optical_constants/asf.html
[46] M. Sacchi, C. F. Hague, L. Pasquali, A. Mirone, J.-M. Mariot, P. Isberg, E. M. Gullikson, and J. H. Underwood, Phys. Rev. Lett. **81**, 1521 (1998).
[47] H.-Ch. Mertins, O. Zaharko, A. Gaupp, F. Schäfers, D. Abramsohn, and H. Grimmer, J. Magn. Magn. Mater. **240**, 451 (2002).
[48] E. Meltchakov, W. Jark, H.-Ch. Mertins, and F. Schäfers, Nucl. Instrum. Methods Phys. Res. A **467-8**, 1411 (2001).
[49] E. Meltchakov, H.-Ch. Mertins, S. DiFonzo, W. Jark, M. Scheer, and F. Schäfers, J. Magn. Magn. Mater. **240**, 550 (2002).